Solar Phys (2011) 273:525–536
DOI 10.1007/s11207-011-9870-y

The Connection of Solar Wind Parameters with Radio and UV Emission from Coronal Holes

D.V. Prosovetsky · I.N. Myagkova

Received: 29 November 2010 / Accepted: 20 September 2011 / Published online: 8 November 2011

Abstract This paper presents the results of a comparison between observations of coronal holes in UV (SOHO EIT) and radio emission (17, 5.7 GHz, 327 and 150.9 MHz, from NoRH, SSRT and Nançay radioheliographs), and solar wind parameters, from ACE spacecraft data over the period 12 March – 31 May 2007. The increase in the solar wind velocity up to $\sim 600\ \mathrm{km\,s^{-1}}$ was found to correlate with a decrease in the UV flux in the central parts of the solar disk. A connection between the parameters of the radio emission from three different layers of the solar atmosphere and the solar wind velocity near the Earth's orbit was discovered. Such a connection is suggestive of a common mechanism of solar wind acceleration from chromospheric heights to the upper corona.

Keywords Corona, quiet · Coronal holes · Radio emission, quiet · Solar wind

1. Introduction

The outward expansion of solar plasma referred to as *'solar wind'* by Parker (1958a) has been intensively studied by ground-based and space experiments since the 1950s (*e.g.*, Biermann, 1951, 1952, 1957; Vsehvyatskiy *et al.*, 1955; Parker, 1958a, 1958b; Licht, 1960; Harrison, 1961; Yallop, 1961; Gringauz *et al.*, 1962; Neugebauer and Snyder, 1966). The solar wind consists of three components – the slow, the fast and the sporadic ones. The existence of different components of the solar wind has been revealed through the observations of the *Mariner-2* spacecraft (Neugebauer and Snyder, 1966). According to Sheeley *et al.*

Energy Storage and Release through the Solar Activity Cycle – Models Meet Radio Observations
Guest Editors: Christophe Marqué and Alexander Nindos

D.V. Prosovetsky (✉)
The Institute of Solar-Terrestrial Physics SB RAS, Irkutsk, Russia
e-mail: proso@iszf.irk.ru

I.N. Myagkova
Lomonosov Moscow State University Skobeltsyn Institute of Nuclear Physics, MSU SINP, Moscow, Russia
e-mail: irina@srd.sinp.msu.ru

(1985), the sporadic component is related to coronal mass ejections. Unlike the sporadic component, the slow and fast components are regular: the slow one exists always, and the fast one is observed periodically. Sources of the latter are coronal holes (CHs) – regions of a unipolar magnetic field with an open configuration (Hundhausen, 1972).

The slow and fast SW components do not only differ in plasma velocity (up to 450 and 800 km s^{-1}, respectively). According to observations of radio scintillations due to inhomogeneities of the interplanetary medium, one of the main SW parameters – the velocity distribution depending on the distance from the Sun – is different for the slow and fast components. The maximum velocity of the slow component is reached at a distance of more than 10 solar radii (Wang *et al.*, 1998), whereas the fast component reaches its maximum velocity near the Sun, at a distance of one or two solar radii (Grall, Coles, and Klinglesmith, 1996). These findings suggest that the mechanism accelerating SW particles is either completely different or has essentially different parameters for different components. Differences in conditions of the fast SW component acceleration are likely to be found at distances of less than one solar radius above the photosphere.

This assumption is also supported by observations of the non-thermal velocity component made with the use of the SUMER UV spectrograph on board SOHO (Wilhelm *et al.*, 1995). Investigation of the ultraviolet spectrum of the CH atmosphere (Chae, Hle, and Lemaire, 1998) shows that the maximum of the fluctuation velocity (*i.e.*, the non-thermal component δV in $V_{\text{solar}} = \sqrt{\frac{2kT}{M} + \delta V^2}$, where k is the Boltzmann constant, T is the ion temperature and M is the mass of the ion emitting the line) is reached at CH levels in the solar atmosphere with temperatures of about 10^5 K (in the transition region). The non-thermal velocity component specifies wave flux $F_{\text{wave}} = \rho \langle \delta V^2 \rangle V_{\text{A}}$, where ρ is the plasma density, V_{A} is the Alfvén velocity. Alfvén waves are probably responsible for acceleration of SW particles and heating of the corona in CH (Cranmer, 2004).

Consequently, parameters of the fast SW component may be formed in the lower solar atmosphere (chromosphere, transition region and lower corona). Some authors also confirm that SW parameters and the solar emission in the optical and UV wavebands are related (*e.g.*, Vršnak, Temmer, and Veronig, 2007; Obridko *et al.*, 2009). The intensity of areas and ratio of areas of CH emission/absorption lines were proposed in the paper of Stepanian *et al.* (2008), Shugai, Veselovsky, and Trichtchenko (2009), Obridko *et al.* (2009) to predict the SW characteristics. However, these methods are generally based on the emission analysis at a single wavelength (sometimes at two wavelengths); *i.e.*, they do not completely reflect the distribution of the plasma parameters and energy release processes in the solar atmosphere.

Supplementary information about the characteristics of the acceleration of the fast SW component could be gained from a thorough study of the UV and radio emission of CH, obtained with high spatial resolution. However, there are only a few papers (*e.g.*, Chae, Hle, and Lemaire, 1998) devoted to spectral observations of the UV emission obtained from SUMER data. This is because of the limitations of the observing programmes of this instrument. Besides, no studies of the dependence between the high-speed SW characteristic and the radio CH emission have been made so far.

Previously, various scientific groups made observations of the radio CH emission over a wide frequency range. Comparative analysis of such observations shows that the frequency range 6 – 17 GHz is characterised by an increased emission (compared to the quiet Sun). This fact cannot be explained by typical models of the solar atmosphere (Maksimov *et al.*, 2006). The *Nobeyama Radioheliograph* (NoRH, 17 GHz, Nakajima *et al.*, 1994) regularly observes an increased level of brightness temperatures in CH (Gopalswamy *et al.*, 1999; Nindos, Kundu, and White, 1999; Moran *et al.*, 2001). Analysis of simultaneous observations with NoRH and the *Siberian Solar Radio Telescope* (SSRT, 5.7 GHz, Grechnev *et al.*,

2003) revealed a linear anticorrelation between brightness temperatures at 5.7 and 17 GHz in the CH regions (Krissinel *et al.*, 2000). According to the results of observations near the solar limb, carried out at SSRT and NoRH, such regions are radially stratified (Maksimov *et al.*, 2004). Analysing observations of the microwave emission, Maksimov *et al.* (2006) showed that the corona (at least, in some parts of the CH) is heated by the wave flux propagating from the photosphere, and the heights where the increased radio emission is formed correspond to the heights of the chromosphere and transition region. Some researchers (see Cranmer, 2004) consider the same mechanisms for the SW acceleration and coronal heating. Observations of the UV spectrum imply a possible connection between energy release and microwave emission in the lower solar atmosphere.

According to the study of the magnetic field configuration of CH, there is a connection between SW characteristics and the so-called "superradial" divergence of magnetic tubes. "Superradial" divergence is determined by measurements of the photospheric magnetic field and its extrapolation (in the potential approximation) to the source surface (Wang and Sheeley, 1990). There is also a connection between SW characteristics and the unipolar field area at the CH base (Eselevich *et al.*, 2009). Forecasting SW parameters using the findings from these studies does not always yield correct results. Probably the magnetic field configuration cannot completely determine the plasma density and velocity of SW, since the SW plasma carries frozen-in magnetic flux out to the outer solar atmosphere and thus changes its configuration. This restricts the application of the magnetic field extrapolation (both potential and non-potential), which does not take this effect into account when forecasting SW parameters.

The purpose of this paper is to study a possible connection between the SW velocity and emission of the lower solar atmosphere of the CH.

2. Observations

2.1. Data

The period from 12 March to 31 May 2007 (during the last solar minimum) was studied. We chose this interval because of the fact that the main parameters of the fast SW component during a solar minimum are defined by characteristics of the CH. Besides, there was a complete set of experimental data available for this period.

To perform the analysis, we used radio images of the Sun recorded by NoRH, SSRT and *Nançay Radioheliograph* at 17 GHz, 5.7 GHz, 327 MHz and 150.9 MHz, and also SOHO/EIT data at the wavelength of the Fe XII line, $\lambda = 195$ Å. Variations in SW parameters were measured by SWEPAM (*Solar Wind Electron, Proton and Alpha Monitor*) on board the ACE spacecraft (*Advanced Composition Explorer*) orbiting near the libration point L1 in the Sun–Earth system (1.5 million km from the Earth toward the Sun), see http://cdaweb.gsfc.nasa.gov/istp_public.

2.2. Data Processing

We determined the UV emission characteristics of CH using a technique similar to the one developed by Vršnak, Temmer, and Veronig (2007). This method implies the determination of fractional CH areas in central meridional slices of the solar disc. Then, the UV emission flux was calculated in this region. We noticed, however, that the polar regions did not contribute significantly to the SW stream registered near the Earth. Thus the region (unlike in

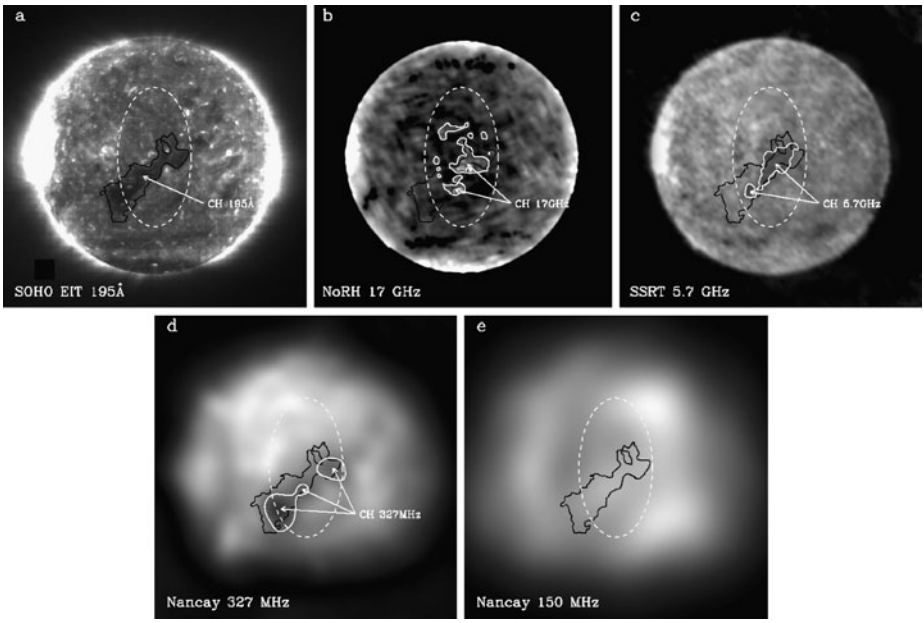

Figure 1 Example of the CH boundary location in the UV and radio emission at four frequencies on 22 March 2007. (a) CH boundaries in the central part of the solar disc with density below $1 \cdot 10^9$ cm^{-3} in the Fe XII band, around $\lambda = 195$ Å. (b – e) Brightness temperatures of the radio emission in the central part of the solar disc (white contour). (b) Above 10^4 K at 17 GHz as deduced from NoRH observations. (c) Below $1.6 \cdot 10^4$ K at 5.7 GHz as deduced from SSRT observations. (d) Below $6.3 \cdot 10^5$ K at 327 MHz as deduced from Nançay radioheliograph observations. (e) The radio emission at 150.9 MHz as deduced from Nançay radioheliograph observations. At this frequency, depression of the radio emission connected with a coronal hole is not observed. CH contours from UV data are overplotted on radio images (see Figure 2a, black contour).

Vršnak, Temmer, and Veronig, 2007) was bounded by the ellipse $R_\odot^2 = X^2 + \frac{Y^2}{1.9}$, where $R_\odot$ is the solar radius. The relation between the semiaxes of the ellipse was determined when comparing positions of CH boundaries and the SW velocity at the point L1 (*i.e.*, we were trying to find out if the high-speed SW stream was registered from a CH that had the latitude and longitude corresponding to the occurrence of a CH boundary on the ellipse boundaries).

The SOHO/EIT data were processed using *SolarSoft* procedures and images from the calibration database of the instrument. The ratio of the emission flux to the CH area (*i.e.*, the average emission flux in the line of Fe XII, $\lambda = 195$ Å) was determined for the CH within the limits of an elliptic central region. The plasma electron density N_e in the CH was deduced from the relationship

$$N_{\mathrm{e,CH}} = 8.34 + 0.509 \cdot \log(I_{\mathrm{EIT}}) \tag{1}$$

obtained in Brosius *et al.* (2002), where I_{EIT} is the Fe XII $\lambda = 195$ Å line intensity of the calibrated image.

We selected pixels with values of the plasma electron density below $1 \cdot 10^9$ cm^{-3} in the central elliptic area of the solar disc for all images. The specific value of the density was obtained by dividing the plasma electron density sum by the number of such pixels. The procedure allowed us to exclude the points corresponding to the bright features located in the elliptic area. Figure 1a, for example, exhibits images of the equatorial coronal hole in the

Fe XII $\lambda = 195$ Å line acquired on 22 March 2007; their boundaries are shown by contour. A coronal bright point in the northwestern part of the CH with plasma electron density over $1 \cdot 10^9$ cm^{-3} was excluded from the CH boundaries. We thus obtained the variation of the UV emission in the CH with a temporal resolution of about 12 minutes (see Figure 2d).

Figure 1(b – e) presents examples of the CH radio emission at 17, 5.7 GHz, 327 and 150.9 MHz. The contours separate CH boundaries and the quiet Sun. At 17 GHz (Figure 1b), the emission of the coronal hole is brighter; at 5.7 GHz (Figure 1c) and 327 MHz (Figure 1d), the CH is darker than the quiet Sun. Referring to Figure 1(b – d), some parts of the CH within the Fe XII $\lambda = 195$ Å line boundaries produce radio emission at 17 GHz, 5.7 GHz and 327 MHz, which is inhomogeneously distributed on the CH surface. At 150.9 MHz, the coronal hole almost equals the level of the quiet Sun. The radio emission at 150.9 MHz can sometimes be brighter or darker than the quiet Sun in the boundaries of the CH in the line of Fe XII with $\lambda = 195$ Å.

Since the CH radio emission in CH boundaries in 195 Å is irregular, we determined the increment/decrement of the normalised flux of the CH in units of the quiet Sun, relative to the quiet Sun level in the regions inside the ellipse:

$$F_{\mathrm{CH},\nu} = \frac{\sum_{i=1}^{n_{\mathrm{CH}}} (T_{\mathrm{B}\nu,i} - T_{\mathrm{QS}\nu,i})}{\sum_{j=1}^{m} T_{\mathrm{QS}\nu,j}}, \tag{2}$$

where ν is the frequency, $T_{\mathrm{B}\nu,i}$ is the brightness temperature inside a CH (its summation is made over elements S_i of the radio CH surface), $T_{\mathrm{QS}\nu,i}$ and $T_{\mathrm{QS}\nu,i}$ are the brightness temperatures of the quiet Sun. The brightness temperature of the quiet Sun is constant for each frequency, $T_{\mathrm{QS},17} = 10^4$ K (Nakajima *et al.*, 1994), $T_{\mathrm{QS},5.7} = 1.6 \cdot 10^4$ K (Grechnev *et al.*, 2003), $T_{\mathrm{QS},327} = 6.3 \cdot 10^5$ K and $T_{\mathrm{QS},150.9} = 6 \cdot 10^5$ K (Mercier and Chambe, 2009). Summation in the denominator is made throughout the disc (the summation index is j; the number of the entire solar disc pixels is m); its result is constant for each frequency. Summation in the numerator is made for image pixels inside the CH, with emission enhancement at 17 GHz and emission depression at 5.7 GHz, 327 and 150.9 MHz, relative to the quiet Sun level (the summation index is i; the number of CH pixels in radio is n_{CH}). So we obtained data of the normalised radio emission flux of the CH from four atmospheric levels, along with data of the plasma electron density inside the CH.

3. Experimental Data Analysis

3.1. Solar Wind Parameters

The three upper panels (a, b, c) of Figure 2 show SW parameter variations during the period under study: the strength of the B_z component and B of the interplanetary magnetic field (IMF), the SW velocity, V_{SW}, and the proton number density N_{p} in SW, respectively. Referring to Figure 2, ten high-speed SW streams (whose beginning is marked by vertical lines) are evident throughout this period. The first SW stream (with its maximum on 13 March) was excluded from consideration, since this SW stream was generated by a CH that had passed through the central meridian some days before 13 March (when the EIT started its observations after regular maintenance service). The lack of EIT data (139 – 145 DOY) was caused by SOHO/EIT maintenance operations during these days. In Figure 2, the streams under consideration in this work are numbered from 1 to 9.

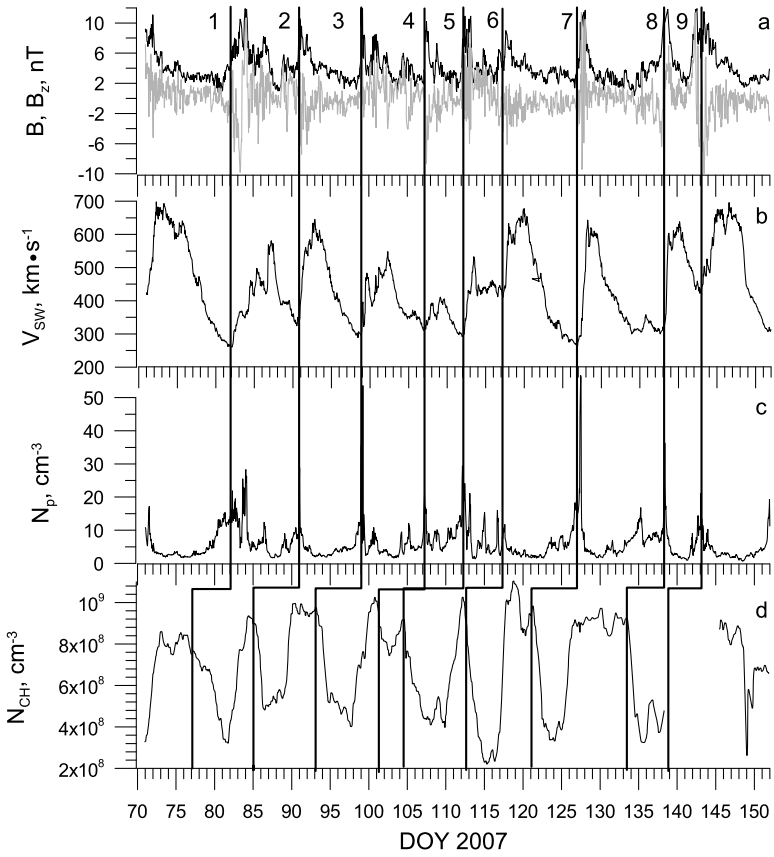

Figure 2 SW parameters measured at L1 in the period 12 March – 31 May 2007: modulus B (black line) and the B_Z component (grey line) of IMF (a); the SW velocity V_{SW} (b); the proton number density N_p (c). Panel (d) shows the variation of the plasma density in the CH, N_{CH} (the curve discontinuity corresponds to the break in the SOHO EIT observations). The x-coordinate is the number of days, starting from 1 January (DOY). Vertical lines correspond to the leading edge of the SW velocity variation and to the leading edge of plasma density decrease due to the CH.

The high-speed streams observed during the period under study have essentially different characteristics: the maximum speed varies from 300 to 700 km s^{-1}, the proton number density at the leading edge of the high-speed stream can reach 40 – 45 cm^{-3} or can be less than 5 cm^{-3} (Figure 2b, c). The variations in the average IMF value B for nine SW streams look similar: we have an abrupt increase at the leading edge of the SW stream and subsequent gradual decrease. During the period under study, B varied in the range from 2 to 10 nT.

3.2. UV Emission of CH

Panel (d) of Figure 2 shows the variation of the plasma density in the CH. It is observed from the figure that the main increases in the SW velocity (1 – 9), taking account of the arrival time at L1, coincide with the plasma density decrease in the CH. The decrease in the UV flux values obtained by the method from Section 2.2 starts when the CH appears at the ellipse boundary. Therefore, the time delay in the arrival of high-speed SW streams is

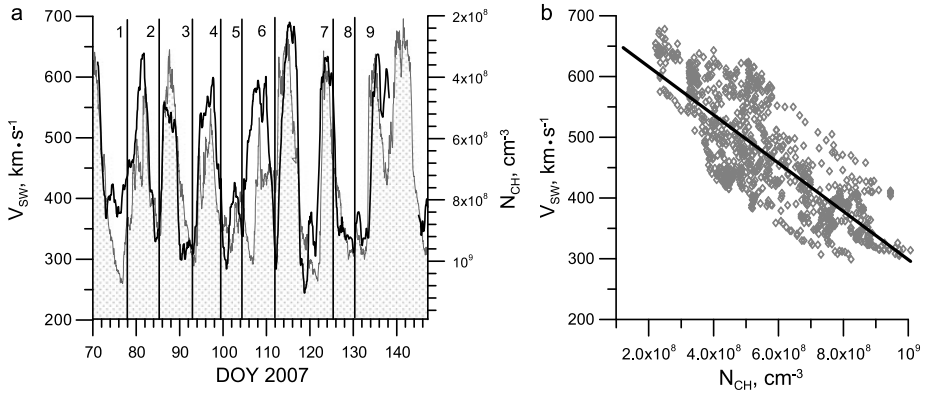

Figure 3 SW velocities at L1 and plasma density in the CH. (a) Superposed variations (shift is 4 days) of density (thick line) and in the SW velocity (filled curve bounded by thin line). The y-axis of the plasma density values is reversed. (b) Correlation between density N_{CH} and velocity V_{SW}, taking into account the different time delays of the SW stream arrival at L1. The line shows best fit to the points.

determined from time differences between the beginning of the leading edge of high-speed stream and the start of decrease in the density related to the CH (see Figures 3a and 3d). The delays were determined from the time difference between the leading edge of density variation associated with the CH and the leading edge of the SW speed variation. The time difference varied from 4 to 7 days. A 5-day delay was used for stream 9 with missing UV data. The data gap was due to SOHO maintenance operations.

In Figure 3a, the diagram of SW velocity variations in time is superposed onto the diagram of the variations in the mean density of the CH, taking into consideration the time delay being equal to the time when SW particles with a propagation velocity of 600 km s^{-1} arrive at L1. The y-axis for the density (to the right) is reversed (*i.e.*, higher values are at the bottom). Referring to Figure 3a, SW velocity variations and plasma density in the CH are similar. The discrepancy between the positions of some SW streams and density depressions (*e.g.*, streams 4, 5 and 6) can be explained by the difference in time of the SW particle arrival at L1.

Taking into account the different delays in the SW particle arrival (from 4 to 7 days; see Figure 2) at the point L1, we show the correspondence between density and velocities $V_{\mathrm{SW}} \geq 300$ km s^{-1} (Figure 3b). The slow SW component is thus cast out in the time series where possible. The values N_{CH} and V_{SW} in eight SW streams are approximated by the linear dependence

$$V_{\mathrm{SW}} = -3.97 \cdot 10^{-7} N_{\mathrm{CH}} + 695 \tag{3}$$

with a correlation 0.63. Notice that the parameters of different SW streams significantly differ (especially the delay time between the plasma density decrease in the CH and the arrival of the SW high-speed stream at the Earth). The correlation of each separate SW stream velocity with its corresponding linear dependence reaches 0.8 – 0.9. However, there was no evidence of correlation between the plasma density in the CH and the proton density in the SW.

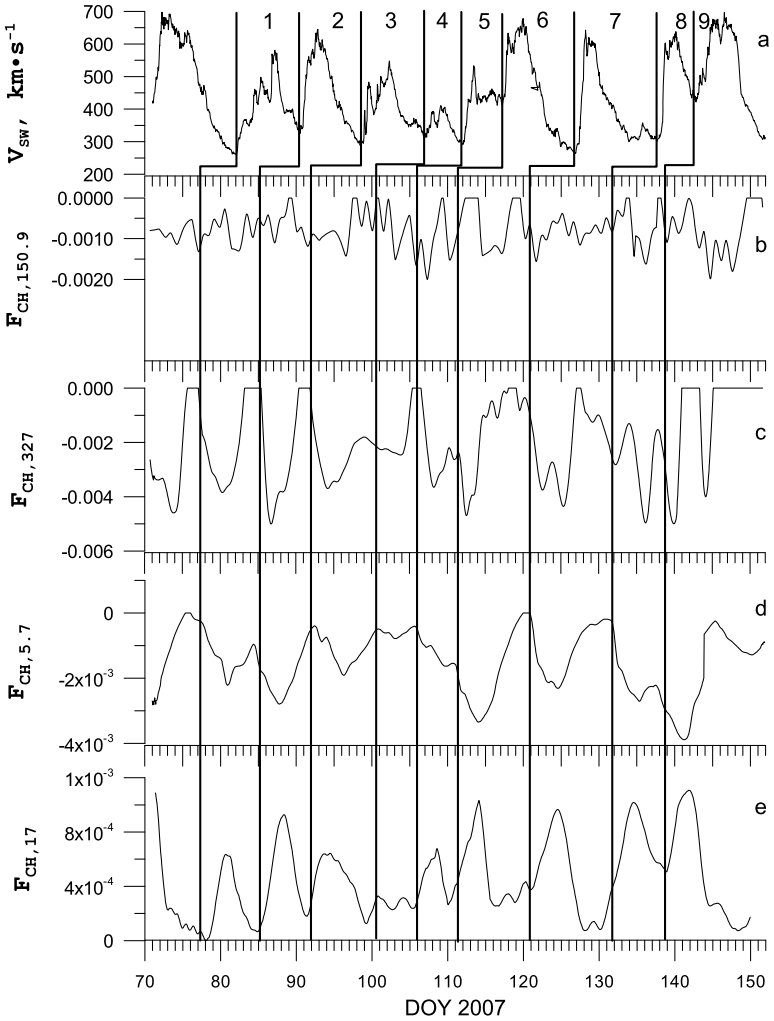

Figure 4 Normalised radio emission fluxes of the CH at 150.9 MHz, 327 MHz, 5.7 and 17 GHz (b, c, d, e) in the quiet Sun units, compared to the SW velocity (a). Vertical lines correspond to the leading edge of SW streams, to the beginnings of CH flux depressions at 150.9 MHz, 327 MHz and 5.7 GHz, and of increases in the microwave flux at 17 GHz.

3.3. Radio Emission of CH

Figure 4(b – e) presents variations in the normalised radio emission flux F_{CH} of the CH at four frequencies, according to data from the NoRH, SSRT and Nançay radioheliographs. The normalised flux was measured with the use of the method described in Section 2. F_{CH} gives the variation of the CH radio flux in units of the quiet Sun, as compared to the flux of the quiet Sun with the same area; *i.e.*, F_{CH} represents a linear function of the CH radio flux with no contribution from the quiet Sun. The normalised radio flux reflects the change in the CH area and the brightness temperature distribution. Negative and positive sign of the F_{CH} imply depression and enhancement of the radio flux (relative to the quiet Sun level),

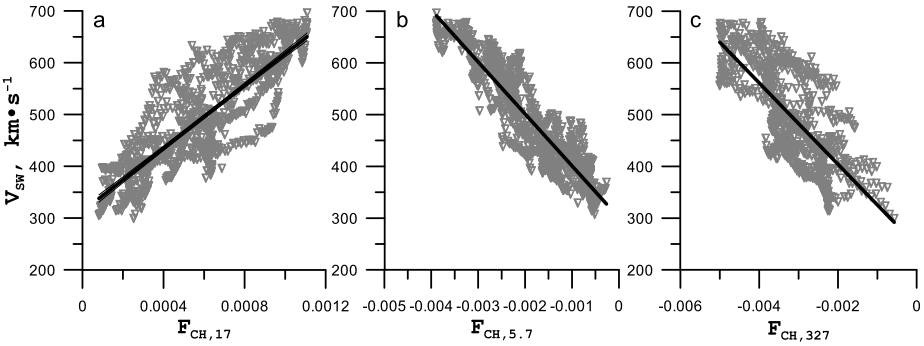

Figure 5 Correlations between the normalised radio flux of CHs at 17 GHz (a), 5.7 GHz (b) and 327 MHz (c) and the SW velocity at L1. Lines show the best fit for the corresponding dataset.

respectively. Vertical lines in Figure 4a mark the beginning of the leading edges of SW streams; those in Figure 4(b – e) the beginning of leading edges of increments/decrements of the normalised radio flux at four frequencies.

The increased radio emission flux (as compared to the quiet Sun) is related to the CH at 17 GHz, whereas the decreased radio emission flux is related to it at 5.7 GHz and 327 MHz. At 150.9 MHz, there is no evidence of an increased nor decreased radio emission flux. Its magnitude is comparable to the flux of neighbouring regions of the solar atmosphere (Figure 4b). Many authors (Dulk and Sheridan, 1974; Trottet and Lantos, 1978; Kosugi, Ishiguro, and Shibasaki, 1986; Borovik *et al.*, 1990; Chiuderi-Drago *et al.*, 1999; Gopalswamy *et al.*, 1999; Nindos, Kundu, and White, 1999; Krissinel *et al.*, 2000; Moran *et al.*, 2001; Maksimov *et al.*, 2006) indicated the increase of the microwave emission at frequencies near 17 GHz, the decrease of the radio emission at frequencies below 5 GHz and above 150.9 MHz, and the drastic decrease in the CH contrast relative to the quiet Sun at frequencies below 150.9 MHz.

Nine CHs were registered during the period under study; time of the SW stream arrival at the point L1 was taken into consideration (Figure 4), and normalised radio emission fluxes with SW velocities $V_{SW} \geq 300$ km s^{-1} were compared at four frequencies (Figure 5a – c). The following relations were obtained from the linear approximation of the experimental data:

$$V_{SW} = 3.04 \cdot 10^5 F_{CH,17} + 313, \tag{4}$$

$$V_{SW} = -1.00 \cdot 10^5 F_{CH,5.7} + 300, \tag{5}$$

$$V_{SW} = -7.85 \cdot 10^4 F_{CH,327} + 247. \tag{6}$$

Observational data correspond to these relations with a correlation of 0.69 at 17 GHz, 0.84 at 5.7 GHz and 0.60 at 327 GHz. No reliable dependence was found for 150.9 MHz. Except for a linear approximation, we also tried other ones, however, the linear fit provided the best correlation. The scatter of flux values could be caused by the noise of antennas and receivers of the radio telescopes, and also by different methods for restoring radio data and the technique for defining UV and radio flux. The difference in methods for processing and restoring radio data has probably caused a difference in correlation coefficients for data obtained at 17 GHz, 5.7 GHz and 327 MHz.

4. Discussion

When analysing experimental data in the previous section, we also examined a probable connection between the other SW parameters (B, B_Z, N_p) and the CH atmosphere characteristics (the radio emission flux F at four frequencies, the UV intensity and its related plasma electron density N_CH). No reliable relations were revealed. Probably these SW parameters obtain their terminal values at other atmospheric levels of the CH or in interplanetary space.

Among the SW parameters under study, we found dependencies only between its velocity at L1 and characteristics of the solar atmosphere emission in the UV and radio bands at three frequencies. Some authors (*e.g.*, Vršnak, Temmer, and Veronig, 2007; Obridko *et al.*, 2009) have already called attention to the relation between SW stream speeds and some characteristics of the UV emission (for instance, the area) in the CH. In this study, we established the dependence of the SW velocity on the mean plasma density in the CH and the radio flux at three frequencies.

According to the linear dependencies $V_\mathrm{SW}(N_\mathrm{CH})$ (3), $V_\mathrm{SW}(F_\mathrm{CH,17})$ (4), $V_\mathrm{SW}(F_\mathrm{CH,5.7})$ (5) and $V_\mathrm{SW}(F_\mathrm{CH,327})$ (6), all CH characteristics (N_CH, $F_{\mathrm{CH},\nu}$) and the SW velocity V_SW are interrelated. Actually, the dependencies $N_\mathrm{CH}(V_\mathrm{SW})$, $F_\mathrm{CH,17}(V_\mathrm{SW})$, $F_\mathrm{CH,5.2}(V_\mathrm{SW})$ and $F_\mathrm{CH,327}(V_\mathrm{SW})$ obtained from Equations (3), (4), (5) and (6) lead to the following relations:

$$\begin{cases} N_\mathrm{CH} = -2.52 \cdot 10^6 V_\mathrm{SW} + 1.75 \cdot 10^9, \\ F_\mathrm{CH,17} = 3.29 \cdot 10^{-6} V_\mathrm{SW} - 1.03 \cdot 10^{-3}, \\ F_\mathrm{CH,5.7} = -1.00 \cdot 10^{-5} V_\mathrm{SW} + 3.00 \cdot 10^{-3}, \\ F_\mathrm{CH,327} = -1.27 \cdot 10^{-5} V_\mathrm{SW} + 3.15 \cdot 10^{-3} \end{cases} \tag{7}$$

and all variables of this system are also linearly dependent. This result confirms a linear dependence between brightness temperatures at 5.7 and 17 GHz in the CH, revealed by Maksimov *et al.* (2006). Notice that no dependence between the SW velocity and the radio emission flux was found for 150.9 MHz at four frequencies. The radio emission flux at this frequency is therefore linearly independent of the emission at the other three frequencies and of the plasma density determined from the Fe XII $\lambda = 195$ Å line emission.

The exact height of the Fe XII $\lambda = 195$ Å line formation in the CH is unknown. Though this line is considered to be coronal, CH limb observations show (according to SOHO EIT data) that the line intensity (and comparable values of plasma density in the CH within the range from 10^7 cm^{-3} to 10^9 cm^{-3}) is observed at heights less than one solar radius. This suggests that plasma density values in the CH obtained in this study correspond to the range of heights where the radio emission is formed at 17 GHz (chromosphere), 5.7 GHz (low corona) and 327 MHz (corona). So we can expect that there will be a frequency or a range of frequencies whose formation heights would correspond to the Fe XII $\lambda = 195$ Å line emission height, and there may be a linear dependence for these frequencies between the emission flux from the CH and the SW velocity. We can also expect that the height of one out of three frequencies under consideration is close to the Fe XII $\lambda = 195$ Å line formation height.

Observations of the CH at 17 GHz (Gopalswamy *et al.*, 1999; Nindos, Kundu, and White, 1999), where the brightness temperature of the CH is higher than that of surrounding quiet regions, confirm energy release in the upper chromosphere and transition region. Besides, observations of the CH at frequencies near 17 GHz also demonstrate an increased brightness temperature in the CH (Gopalswamy *et al.*, 1999; Nindos, Kundu, and White, 1999; Krissinel *et al.*, 2000; Moran *et al.*, 2001; Maksimov *et al.*, 2006).

The connection between the solar atmosphere parameters and high-speed solar wind is evident at heights less than one solar radius; at heights more than one solar radius, no dependence is observed. This is confirmed by the absence of a connection between the radio emission flux in the CH at 150.9 MHz and the velocity of the high-speed SW, whereas such a connection is evident at higher frequencies. The papers of Dulk and Sheridan (1974), Chiuderi-Drago (1974), Trottet and Lantos (1978), Chiuderi-Drago *et al.* (1999) also show that the CH at $\sim$150.9 MHz and below may be invisible on the quiet Sun background, or their brightness temperature may slightly differ from the temperature of the quiet Sun.

The established connection between SW parameters and radio emission established in this work provides a good reason to believe that the acceleration process of the high-speed SW and characteristics of the solar atmosphere are related at heights less than one solar radius. Some authors (Hollweg, 1978; Tu, Zhou, and Marsch, 1995; Tu *et al.*, 2005; Suzuki and Inutsuka, 2006) think that the acceleration of SW particles is caused by the energy transfer from the wave flux to them (for instance, due to the wave – particle resonance), and wave sources are in the lower solar atmosphere. According to data from the SUMER instrument on board SOHO (Chae, Hle, and Lemaire, 1998), the maximum value related to the wave flux is in the transition region. Measured wave velocities in the polar CH are about 130 – 160 km s^{-1} (already in the chromosphere and transition region) and up to 330 km s^{-1} in the lower corona, according to data from the instruments of *Hinode*/EIS and SOHO/SUMER instruments (Gupta *et al.*, 2010). This implies that the particle acceleration in the high-speed SW related to the CH is observed already in the lower solar atmosphere, and within this framework, the connection of the SW velocity near the Earth's orbit with the emission at these heights becomes clear.

Measurements of plasma velocity with UV coronal spectrographs may reveal whether SW particles at coronal heights are accelerated or not. However, no studies on this issue have been published so far. We hope that this issue will be addressed with data from new space observatories (*e.g.*, Solar C).

5. Summary

From the analysis of available observational data, the following conclusions have been drawn.

i) The velocity of the high-speed SW during the period under study is related to the mean emission intensity of the Fe XII line with $\lambda = 195$ Å (and the mean plasma density N_{CH} determined from it) in the CH.
ii) The density has been established between velocity of the high-speed SW and CH radio emission flux in the chromosphere and lower corona during the period under investigation.

Acknowledgements We are grateful to the team of observatories SOHO (instrument EIT), SSRT, Nobeyama and Nançay for providing free access to the data, which enabled this work.

References

Biermann, L.: 1951, *Z. Astrophys.* **29**, 274.
Biermann, L.: 1952, *Z. Naturforsch.* **7a**, 127.
Biermann, L.: 1957, *Observatory* **77**, 109.
Borovik, V.N., Kurbanov, M.S., Livshits, M.A., Ryabov, B.I.: 1990, *Sov. Astron.* **34**(5) 522.

Brosius, J.W., Landi, E., Cook, J.W., Newmark, J.S., Gopalswamy, N., Lara, A.: 2002, *Astrophys. J.* **574**, 453.
Chae, J., Hle, U.S., Lemaire, P.: 1998, *Astrophys. J.* **505**, 957.
Cranmer, S.R.: 2004, In: Walsh, R.W., Ireland, J., Danesy, D., Fleck, B. (eds.) *Proceedings of the SOHO 15 Workshop – Coronal Heating* **SP-575**, European Space Agency, Paris, 154.
Chiuderi-Drago, F.: 1974, In: G. Righini (ed.) *Skylab Solar Workshop: Osserv. Mem. Oss. Astrofis. Arcetri* **164**, 242.
Chiuderi-Drago, F., Landi, E., Fludra, A., Kerdraon, A.: 1999, *Space Sci. Rev.* **87**(1–2), 141.
Dulk, G.A., Sheridan, K.V.: 1974, *Solar Phys.* **36**, 191.
Eselevich, V.G., Fainshtein, V.G., Rudenko, G.V., Eselevich, M.V., Kashapova, L.K.: 2009, *Cosm. Res.* **47**, 95.
Grall, R.R., Coles, W.A., Klinglesmith, M.T.: 1996, In: *Proc. of the 8th International Solar Wind Conference: Solar Wind Eight*, *AIP Conf. Proc.* **382**, 108.
Gopalswamy, N., Shibasaki, K., Thompson, B.J., Gurman, J., DeForest, C.: 1999, *J. Geophys. Res.* **104**(A5), 9767.
Grechnev, V.V., Lesovoi, S.V., Smolkov, G.Y., *et al.*: 2003, *Solar Phys.* **216**(1), 239.
Gringauz, K.I., Bezrukikh, V.V., Ozerov, V.D., Rybchinskii, R.E.: 1962, *Planet. Space Sci.* **9**(3), 103 (First published: 1960, *Dokl. Acad. Sci. USSR* **131**, 1301).
Gupta, G.R., Banerjee, D., Teriaca, L., Imada, S., Solanki, S.: 2010, *Astrophys. J.* **718**, 11.
Harrison, E.R.: 1961, *Nature* **189**, 993.
Hollweg, J.V.: 1978, *Rev. Geophys. Space Phys.* **16**, 689.
Hundhausen, A.J.: 1972, *Coronal Expansion and Solar Wind*, Springer, Berlin.
Kosugi, T., Ishiguro, M., Shibasaki, K.: 1986, *Publ. Astron. Soc. Japan* **38**(1), 1.
Krissinel, B.B., Kuznetsova, S.M., Maksimov, V.P., Prosovetsky, D.V., Grechnev, V.V., Stepanov, A.P., Shishko, L.F.: 2000, *Publ. Astron. Soc. Japan* **52**, 909.
Licht, A.L.: 1960, *J. Geophys. Res.* **65**(5), 1397.
Maksimov, V.P., Prosovetsky, D.V., Kuznetsova, S.M., Obukhov, A.G.: 2004, *Solar-Terr. Phys.* **6**, 80.
Maksimov, V.P., Prosovetsky, D.V., Grechnev, V.V., Krissinel, B.B., Shibasaki, K.: 2006, *Publ. Astron. Soc. Japan* **58**(1), 1.
Mercier, C., Chambe, G.: 2009, *Astrophys. J.* **700**, L137.
Moran, T., Gopalswamy, N., Dammasch, I.E., Wilhelm, K.A.: 2001, *Astron. Astrophys.* **378**, 1037.
Nakajima, H., Nishio, M., Enome, S., Shibasaki, K., Takano, T., Hanaoka, Y., Torii, C., Sekiguchi, H., *et al.*: 1994, *Proc. IEEE* **82**(5), 705.
Neugebauer, M., Snyder, C.W.: 1966, *J. Geophys. Res.* **71**, 4469.
Nindos, A., Kundu, M.R., White, S.M.: 1999, *Astrophys. J.* **527**(1), 415.
Obridko, V.N., Shelting, B.D., Livshits, I.M., Asgarov, A.B.: 2009, *Solar Phys.* **260**, 191.
Parker, E.: 1958a, *Astrophys. J.* **128**, 664.
Parker, E.: 1958b, *Astrophys. J.* **128**, 677.
Sheeley, N.R. Jr., Howard, R.A., Michels, D.J., Koomen, M.J.: 1985, *J. Geophys. Res.* **90**, 163.
Shugai, Yu.S., Veselovsky, I.S., Trichtchenko, L.D.: 2009, *Geomagn. Aeron.* **49**(4), 41.
Stepanian, N.N., Kuzin, S.V., Fainshtein, V.G., Rudenko, G.V., Malashchuk, V.M., Perebeinos, V.A., Shtertser, N.I., Zhigalkin, R.K., *et al.*: 2008, *Solar Syst. Res.* **42**(1), 83.
Suzuki, T., Inutsuka, S.: 2006, *Astrophys. J.* **632**(1), L49.
Trottet, G., Lantos, P.: 1978, *Astron. Astrophys.* **70**, 245.
Tu, C.-Y., Zhou, C., Marsch, E.: 1995, *Space Sci. Rev.* **73**, 1.
Tu, C.-Y., Zhou, C., Marsch, E., Xia, L.-D., Zhao, L., Wang, J.-X., Wilhelm, K.: 2005, *Science* **308**(5721), 519.
Vršnak, B., Temmer, M., Veronig, A.M.: 2007, *Solar Phys.* **240**(2), 315.
Vsehvyatskiy, S.K., Nikol'skiy, G.M., Ponomarev, E.A., Cherednichenko, V.I.: 1955, *Astron. Zh.* **32**(2), 165.
Wang, Y.-M., Sheeley, N.R. Jr.: 1990, *Astrophys. J.* **355**, 726.
Wang, Y.-M., Sheeley, N.R., Walters, J.H. Jr., Brueckner, G.E., Howard, R.A., Michels, D.J., Lamy, P.L., Schwenn, R., Simnett, G.M.: 1998, *Astrophys. J.* **498**, L165.
Wilhelm, K., Curdt, W., Marsch, E., Schuhle, U., Lemaire, P., Gabriel, A., Vial, J.-C., Grewing, M., *et al.*: 1995, *Solar Phys.* **162**, 189.
Yallop, B.D.: 1961, *Observatory* **81**, 235.